Ceramics-Silikáty 66 (2), 218-227 (2022)
www.ceramics-silikaty.cz doi: 10.13168/cs.2022.0016

THE EFFECT OF POZZOLANIC WASTE OF DIFFERENT NATURE ON THE HYDRATION PRODUCTS, STRUCTURE AND PROPERTIES OF HARDENED CEMENT PASTE

#KESTUTIS BARKAUSKAS, DŽIGITA NAGROCKIENE, INA PUNDIENE

Vilnius Gediminas Technical University, Sauletekio av. 11, Vilnius, LT-10223, Lithuania

#E-mail: kestutis.barkauskas@vilniustech.lt

Submitted February 24, 2022; accepted March 24, 2022

Keywords: Ground Waste Glass, Metakaolin, Cement Paste, Microstructure, Compressive Strength

The paper analyses the effect of different pozzolanic waste – ground waste glass, metakaolin and addition made of ground waste glass and metakaolin, on cement hydration and physical-mechanical properties of hardened cement paste. Four batches of specimens were made for the tests. Cement (C) in the cement matrix was replaced with 5 % of ground waste glass (5S), 15 % of metakaolin and mixed pozzolanic was addition (MIX 20) made of 5 % of ground waste glass and 15 % of metakaolin. The best improvement of mechanical properties after 90 days of curing was observed in the specimens modified with the mixed pozzolanic addition. X-ray, TGA tests and microstructure analysis revealed that the improvement of mechanical properties is caused by the higher content of hydration products and a strong contact zone between glass particles and foam glass splinters present in metakaolin waste addition. The formation of C-S-H hydrates on the surface of glass foam splinters and in the pores was also observed. This kind of microstructure formation has a positive effect on cement matrix microstructure and physical-mechanical properties of hardened cement paste.

INTRODUCTION

Concrete production technology has to meet high standards. The following requirements are raised for concrete: durability and quality stability, sustainability, environmental friendliness, high production efficiency, high strength and cost-effectiveness. Additional cement based materials have become an essential component of modern cement and modern concrete [1-6].

The production phase of cement clinker contributes negatively to greenhouse gas emissions and global warming, and has a significant environmental impact. However, the use of supplementary cementitious materials in the construction industry has shown that it is possible to significantly reduce the cement content in concrete. The use of SCMs, as well as ground glass and metakaolin waste, can reduce the need for cement without compromising the strength of concrete. Lower levels of natural sand used in concrete production create a demand for fine aggregates, which can be substituted by crushed glass waste. The growing demand for supplementary cementitious materials is leading industry and academia to look for more practical alternatives, such as the use of waste glass [7-9].

Decomposition of waste glass in landfills will last for thousands of years due to stable chemical properties of glass. There is evidence that recycling is the best waste glass utilisation technique. Waste glass is composed of silica (SiO_2) and various metal oxides, namely Ca, Al and Fe. XRF analysis conducted by other authors shows that the main component of waste glass is silica, which accounts for more than half (68.9 ± 1 %) of the total mass [10-14].

Fine powder of waste glass helps to optimise the pore size, which increases the density of the concrete. However, the density of concrete decreases with bigger particle size of waste glass (> 150 μm). The right amount of waste glass used can effectively improve the internal microstructure of concrete and increase the content of high density calcium silicate hydrate in the later age, which helps to reduce creep. In theory, waste glass can be fully recycled in a conventional production process, but this is not an easy task due to the complexity of the cleaning, separation and sorting processes. For decades the academic community has been working hard to develop the use of waste glass in the production of building materials [15-17].

The use of glass waste in cementitious composites is limited. With more than 15 % of glass powder added the compressive strength of hardened cement paste falls below the value of the control specimens. It can be explained by the reduction of the cement content in the

material and reduced level of the hydrates (C-S-H and portlandite), which create the design strength of concrete. Properly recycled waste glass can not only increase the durability and compressive strength of concrete, but, when used for partial replacing of cement, can also solve some important environmental, energy and cost issues [18-19].

Metakaolin (MK), $Al_2Si_2O_7$, is a predominantly amorphous dehydration product of kaolinite $Al_2(OH)_4Si_2O_5$ with strong pozzolanic activity. MK is obtained from kaolin clay by calcination at moderate temperatures (650 - 800 °C). At higher temperatures (> 900 °C) metakaolin participates in further reactions to form crystalline compounds. The final products are free silica and mullite. It contains active forms of silica and alumina which will react with CH. The availability of materials and increased durability are main reasons for using clay pozzolans in mortar and concrete. In addition, depending on the firing temperature and the type of clay, it is also possible to increase the strength of concrete, especially in the early stages of curing. The increase in very early strength is due to the combination of aggregate effect and accelerated hydration of the cement. This effect is later enhanced by the pozzolanic reaction between the FC and the CH produced by cement hydration [20-23].

Metakaolin consists mainly of SiO_2 and Al_2O_3 and is highly reactive. The pozzolanic reactivity of waste glass and metakaolin strongly influences the kinetics of hydration reaction of the binder and the properties of the obtained specimens [24-25].

The microstructure of concrete where cement is replaced with 10 % of metakaolin becomes more compact in the early stage, while in the later stage, an appropriate amount of metakaolin can improve the internal bonding of the specimen's microstructure by reducing the pores [26].

Researchers concluded from SEM analysis that the volume of existing C – S – H increases in proportion to the percentage of Portland cement replaced with metakaolin. This relationship was predicted and can be attributed to the pozzolanic reactions of metakaolin and calcium hydroxide, and subsequently better strength and durability of concrete. The microscopic analysis shows that the addition of metakaolin into the cement paste reduces the amount of calcium hydroxide and increases the amount of bound water [27-29].

The aim of the work described in the paper was to investigate the effect of different pozzolanic waste materials, namely ground glass and metakaolin generated in the foam glass production process, on cement hydration products in specimens cured for 90 days, and to evaluate the effect of these additions on the physical and mechanical properties of the cured specimens.

EXPERIMENTAL

Portland cement CEM I 42.5 R, glass powder, and metakaolin were used for the tests. The physical properties of the materials used are given in Table 1.

Table 1. Physical properties.

Properties	CEM I 42.5 R	Glass powder	Metakaolin
Specific surface area [$cm^2 \cdot g^{-1}$]	3700	2514	7036
Particle density [$kg \cdot m^{-3}$]	3200	2500	2147
Bulk density [$kg \cdot m^{-3}$]	1200	850	600

Table 2 presents chemical compositions of cement, glass powder and metakaolin. The pozzolanic activity of glass powder (560 $mg \cdot g^{-1}$) was found to be lower compared to the activity of metakaolin (927 $mg \cdot g^{-1}$).

Table 2. Chemical composition of cement, glass powder and metakaolin.

SiO_2	Al_2O_3	Fe_2O_3	CaO	K_2O	SO_3	Na_2O	TiO_2	MgO	Other
Chemical composition of cement [%]									
20.76	6.12	3.37	63.50	1.00	0.8	0.3	-	-	4.45
Chemical composition of glass powder [%]									
68.15	12.18	1.30	3.95	2.80	-	0.75	0.20	0.90	9.77
Chemical composition of metakaolin [%]									
50.6	34.0	0.74	2.49	0.7	0.07	10.1	0.37	0.59	0.34

Compositions of specimens formed from cement paste are presented in Table 3. The specimens were made by replacing some of the cement with ground waste glass and metakaolin. The water-to-cement (W/B) ratio was kept constant for all specimens and amounted to 0.45.

Table 3. Mixing proportion of cement paste specimens.

Specimen marking by composition	C	S5	M15	MIX20
Metakaolin content [%] (by weight of cement)	0	0	15	15
Glass powder content [%] (by weight of cement)	0	5	0	5
Cement [%]	69	64	54	49
Water [%]	31	31	31	31
Metakaolin [%]	0	0	15	15
Glass powder [%]	0	5	0	5
W/B	0.45	0.45	0.45	0.45

The cement pastes were mixed mechanically using a laboratory mortar mixer. The mixing time was 240 seconds. The mixed paste were poured into standard 40 × 40 × 160 mm moulds and cured for 24 h. After one day, the specimens were disassembled and further cured in water at 20 ± 1.0 °C for 27 and 90 days.

Physical and mechanical characteristics of hardened cement paste were determined according to standard LST EN ISO 1927-6:2013. Density, compressive strength, and flexural strength of the specimens were determined after 28 and 90 days of curing. Five hardened cement paste prisms of 40×40×160 mm dimensions were taken to determine water absorption. Hardened cement paste specimens were dried to constant mass, weighted, soaked in water and weighted in air after 96 h.

A SmartLab (Rigaku) diffractometer was used to determine the phase composition of cement mortar specimens. The XRF-ray diffraction patterns were recorded in the angular range 5 - 75° (2θ), detector step 0.02°, detector movement speed 1° per minute. Database of Crystal Structures PDF- 4+ (2016) was used for automated quantitative analysis.

The microstructure of hardened cement paste, glass powder and metakaolin was determined by means of SEM microscopy. Tests were made using a scanning electron microscopy (SEM) device SEM JEOL 7600.

The thermal stability analysis (DTA/TG) of hardened cement paste specimens was done using the simultaneous thermobalance system STA PT-1600 from Linseis Germany. The temperature of specimens weighting 50 ± 5 mg was raised to 1000 °C at the rate of 10 °C·min^{-1}. using air as the heating environment.

RESULTS AND DISCUSSION

The phase assemblage of hardened cement paste specimens was characterized by XRD after 28 and 90 days of hardening, and the results are presented in Figure 1 and Figure 2. Figures 1 and 2 illustrate X-ray diffraction patterns of control specimen and modified specimen. The changes in the properties of hardened

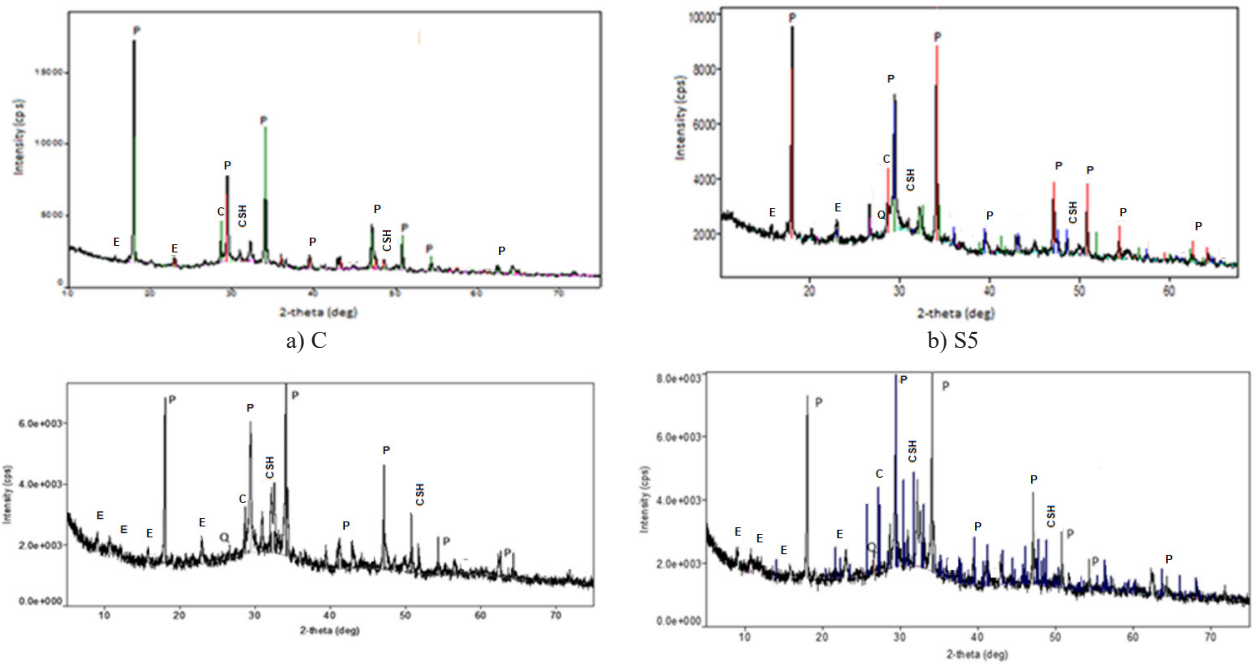

a) C b) S5

c) M15 d) MIX20

Figure 1. X-ray image of hardened cement paste at 28 days.
P- portlandite; E-ettringite; C- calcite; CSH- calcium silicate hydrate; Q- quartz.

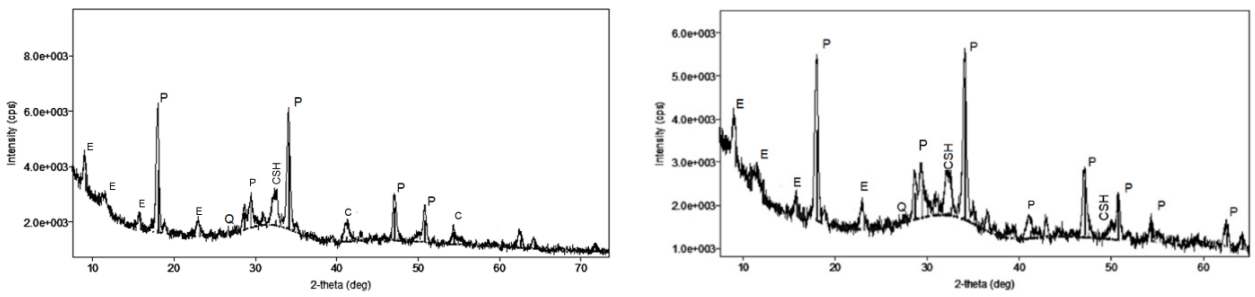

a) C b) S5

Figure 2. X-ray image of cement stone at 90 days.
P- Portlandite; E-Ettringite; C- Calcite; Q- Quartz; CSH-calcium silicate hydrate.

continues on the next page ...

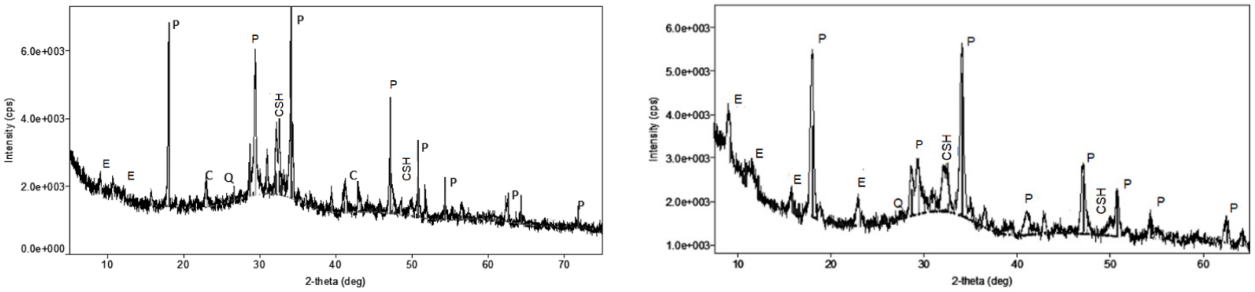

c) M15 d) MIX20

Figure 2. X-ray image of cement stone at 90 days.
P- Portlandite; E-Ettringite; C- Calcite; Q- Quartz; CSH-calcium silicate hydrate.

cement paste specimens with glass and metakaolin addition occur due to phase transformation during hydration processes in hardening cement paste.

Hydration products, such as portlandite, ettringite and CSH, are identified in the control specimen and in specimens with additives cured for 28 days. Free cement minerals C_3S and C_2S are found in the XRD curve. As the amount of cement in the specimens decreases, the amount of portlandite also decreases consistently from 60 % to 49 % when the replacement of cement in the specimens was 20 % (Figure 3). Ettringite formation is observed in all specimens [30]. The biggest amount of ettringite is formed in specimen MIX20, where both additives – metakaolin and glass were used. The lowest amount of ettringite is formed in specimen M15, where only metakaolin is used. The most intense CSH formation occurs in specimen M15 with metakaolin only and in specimen MIX20 with both additives. The amount of calcite also depends on the amount of cement in the composition and tends to decrease because less $Ca(OH)_2$ in specimens is created and it can react with CO_2 from the air [31].

After 90 days of hardening (Figure 2 and Figure 4) the amount of portlandite in the specimens decreases. Less portlandite in specimen MX20 was observed. At the same time the growth of ettringite and CSH is observed. Significant increase of CSH is observed in the specimens M15 and MX20. As was expected, the intensity of CSH peaks increases. Scientists [32] determined that ettringite is not stable without the protective C-S-H gel layers. With the progress of hydration, C-S-H gel with a large specific surface area gradually forms a protective gel layer on the surface of ettringite. This layer resists the diffusion of ions which increase the resistance of ettringite transformation, thereby enhancing the stability of ettringite. Basing on the mentioned studies, it can be concluded that the increase of ettringite is observed due to the growing amount of CSH. It forms the protective layer on the surface of ettringite and stops its transformation into other mineral forms.

The amount of calcite also significantly decreases in compositions, especially when additives were used. The reduction of calcite amount shows that Ca ions participate in the hydration reaction and more hydration products (CSH and ettringite) are formed. It should be mentioned that the CSH amount is three times higher in the composition MX20, than in the control sample, but the amount of ettringite is only 23 % higher. It can be stated that the combined use of metakaolin and glass facilitate hydration process and consequently more hydration products are produced in the system, despite the lower amount of cement in the specimen.

XRD analysis of hardened cement paste specimens was complemented by thermogravimetric analysis. It may be seen that DTA and DTG curves of all specimens have 3 main endothermic effects at temperature intervals of (90 - 200) °C , (450 - 530) °C and (700 - 760) °C (Figure 5). At the temperature interval of (60 - 105) °C,

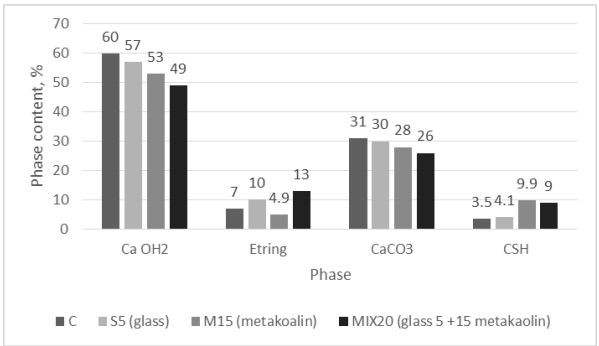

Figure 3. Phase content (%) in the composition after 28 days of hardening.

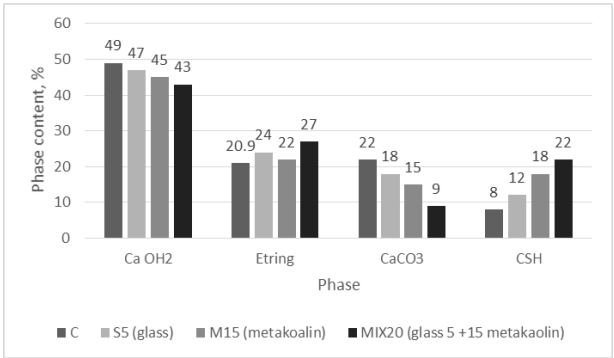

Figure 4. Phase content (%) in the composition after 90 days of hardening.

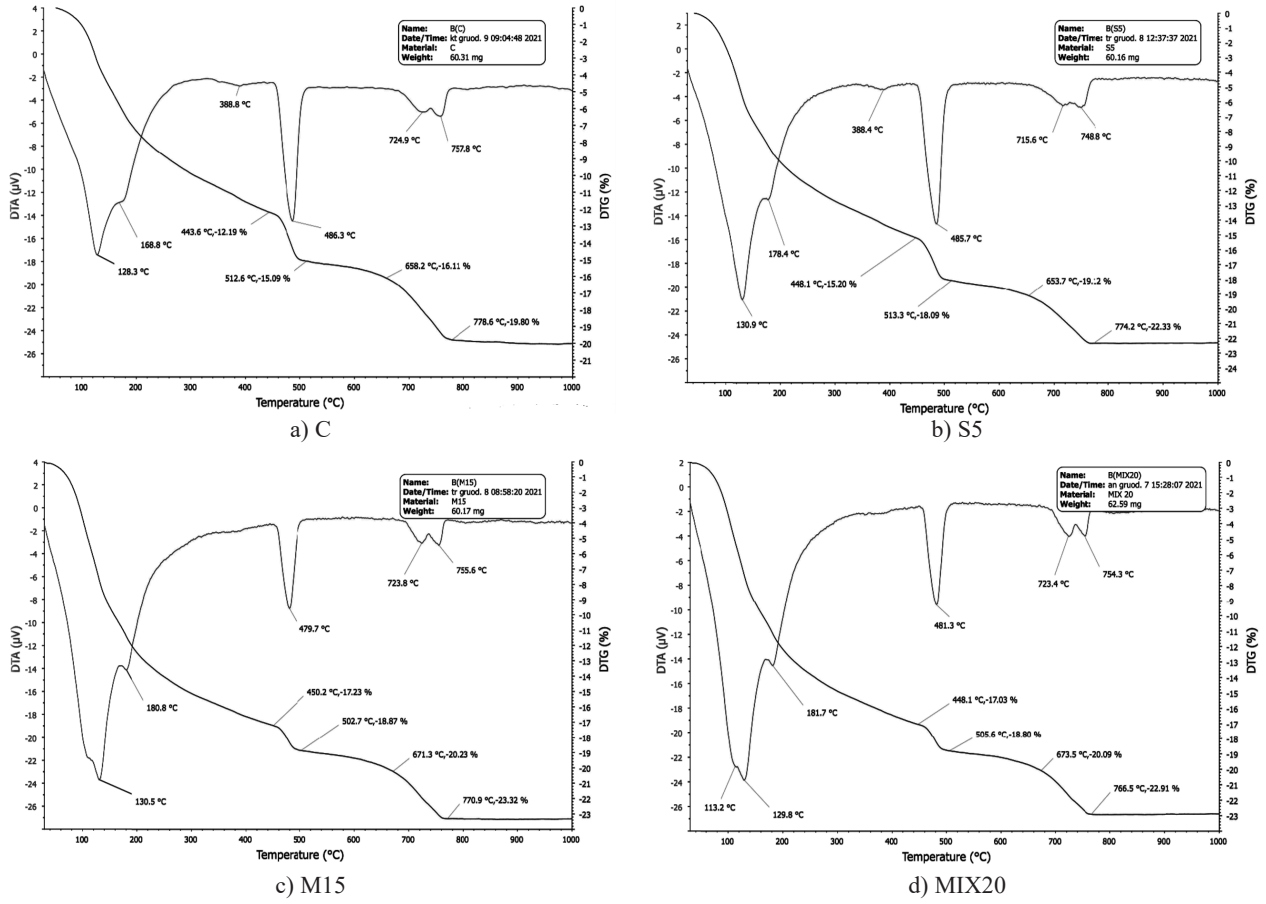

Figure 5. Thermal images of hardened cement paste.

free water and a part of bound water is removed. During the dehydration process, the removal of hydroxyls and water molecules from the structure occurs [33]. It is generally considered that the evaporable water is completely eliminated at 120 °C [34]. At the temperature of (100 - 200) °C [35], the majority of Portland cement mineral hydrates (calcium hydroaluminates, ettringite [36], monocarboaluminates [37], etc.) lose hydrated water. The endothermal effect was observed in the temperature range of (450 - 530) °C. The effect is attributed to the decomposition of portlandite. In the temperature range of (700 - 770) °C, the endothermal effect was observed due to the decomposition of calcite [38]. Mass losses of the specimens during heating in different temperature ranges obtained by means of DTG method are presented in Table 4. It can be concluded that the overall mass loss in the specimens containing additives is by 2.3 % to 3.3 % higher than in the control specimen.

The mass loss in specimens of all four compositions in a defined temperature interval describing a certain effect is presented in Figure 6. The mass loss of physically bound water in the control specimen after 28 days of hardening (up to 90 °C) is 1.0 % (Figure 6). It is assumed that a considerable endothermal effect obtained at 90 °C – 140 °C occurs due to the decomposition of ettringite. These findings are supported by the results reported in literature sources as well as by XRD results (Figure 1). It is known that ettringite can decompose at 80 - 90 °C [39]. Other researchers [35] found that the decomposition of ettringite occurs at (110 – 140) °C. The mass loss of ettringite obtained during decomposition

Table 4. Mass loss expressed in percentage in specimens of different composition determined during the DTG test.

Specimen marking	Mass loss in % in the temperature range up to:						W/S	W/C	Cement content in composition [%]
	90 °C	160 °C	200 °C	530 °C	760 °C	1000 °C			
C	1.0	4.6	7.4	15.8	19.8	20.0	0.34	0.34	100
S5	2.0	6.2	10.1	18.1	22.3	23.3	0.34	0.36	95
M15	2.6	8.4	12.6	18.9	22.3	22.3	0.34	0.46	85
MIX20	3.0	8.4	12.2	18.8	22.9	22.9	0.34	0.44	80

is 3.6 % (Figure 6). At temperature of (160 - 200) °C, the loss of bound water from the decomposition of the CSH occurs [40]. In this case, DTG analysis, which confirms the results of XRD test with the control specimen, shows the mass loss of 2.8 %. Decomposition of portlandite in the thermogram shows the mass loss of 3.0 %. During the decomposition of carbonates the specimen lost 3.7 % of its weight. The overall mass loss was 20.0 %.

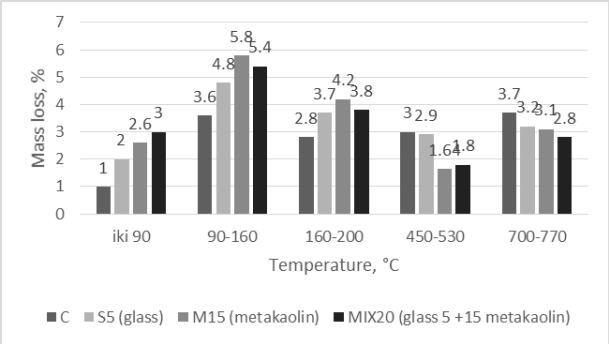

Figure 6. The weight loss of specimens in the defined temperature interval, describing a certain effect.

With the decrease of cement amount in the specimens S5, M15 and MIX20, the amount of unbound water in modified specimens was 2-3 times higher than in the control specimen. The mass loss of specimens M15 and MIX20 was 5.8 % and 5.4 % respectively in the temperature interval of (90 - 160) °C. The amount of ettringite formed in these specimens was 1.6 and 1.33 times higher compared to the control specimen. The weight loss in specimen S5 was 4.8 %. This observation was supported by XRD test results. It is possible that more ettringite was formed due to a higher amount of aluminium in metakaolin. In the temperature interval of (160 - 200) °C, the mass loss in specimens M15 and MIX20 reached 3.8 % and 4.2 %, and 3.7 % in specimen S5. It is obvious that despite the lower cement content in the composition, pozzolanic additives determine more intensive cement hydration and CSH formation in modified specimens compared to the control composition. Compared to the mass loss in control specimen (2.8 %), specimens with pozzolanic additives are characterised by 1.3 - 1.5 times higher amount of CSH. A higher amount of aluminium in metakaolin and SiO_2 in ground glass promotes not only the formation of ettringite but CSH as well.

Decomposition peaks of portlandite show that the most of the portlandite is formed in the control specimen. Presumably it is due to the highest content of cement in the control specimen. The same is proved by the highest portlandite peak intensity in XRD chart.

Less portlandite is formed in the specimens with the decrease of cement amount in the composition. Specimen S5, where 5 % of cement was replaced with ground waste glass, has 3.30 % less portlandite Compared to control specimen. Moreover, the amount of portlandite is 1.8 and 1.66 times lower in specimens M15 and MIX20 where aluminium content is high. It clearly shows that portlandite consumption and CSH formation is strongly accelerated by partial replacement of cement with pozzolanic additives. During decomposition of carbonates, the highest mass loss appeared in the control specimen. With the decrease of cement amount in the composition, the amount of carbonates decreases (from 3.7 % (in control specimen) to 2.8 % (in specimen MIX20). It is assumed that it takes a long time for portlandite to carbonise. As less portlandite is formed in compositions with lower cement content, a lower amount of carbonates was determined in those specimens. The overall mass loss of control specimen was 13 % lower than in the specimens with additives. That shows that pozzolanic additives assure more intensive hydration of cement.

The density of hardened cement paste was tested after 28 and 90 days of curing using the methods described in the methodology chapter. The obtained results are presented in the Table 7. At 28 days, the highest density of 2063 $kg \cdot m^{-3}$ determined in specimens MIX 20 was 1.21 % higher than the density of control specimens, which was 2038 $kg \cdot m^{-3}$. The presumable cause of this difference is a higher amount of hydration products, such as CSH, produced in the specimens containing a mixed pozzolanic additive. CSH has the highest density of 2.6 $kg \cdot m^{-3}$, whereas the density of portlandite is 2.23 $kg \cdot m^{-3}$ and the density of ettringite is 1.8 $kg \cdot m^{-3}$ [41].

At 90 days the density of hardened cement paste specimens slightly increases by 0.008 % – 0.0086 %. Such an increase in density is caused by the crystallisation of new products.

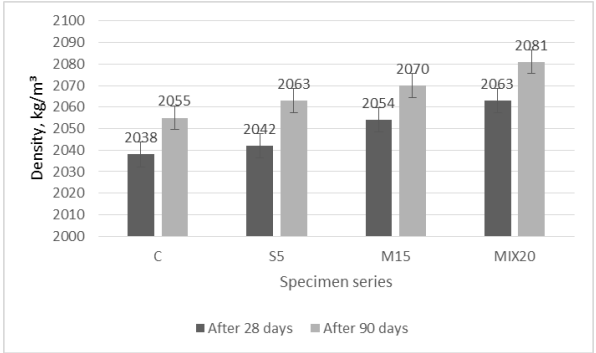

Figure 7. Densities of hardened cement paste at 28 and 90 days .

Figure 8 illustrates the results of ultrasonic pulse velocity (UPV) in hardened cement paste at 28 and 90 days. At 28 days the highest UPV value of 3798 $m \cdot s^{-1}$ was determined in specimens MIX 20 and the lowest value of 3542 $m \cdot s^{-1}$ was determined in control specimens. These results correlate with density test results as the

UPV increases in more compact hardened cement paste. It was found that after 28 days the UPV values in specimens MIX 20, where cement was replaced with 5 % of ground waste glass and 15 % of metakaolin, increased up to 6.74 % compared to the control specimen.

The UPV values were higher in hardened cement paste specimens cured for 90 days. The highest UPV value of 4002 $m \cdot s^{-1}$ was observed in specimen MIX 20 and the lowest value of 3789 $m \cdot s^{-1}$ was recorded in the control specimen. After 90 days of curing, the UPV values in the specimens where cement was replaced with 20 % of pozzolanic waste increased 5.32 %.

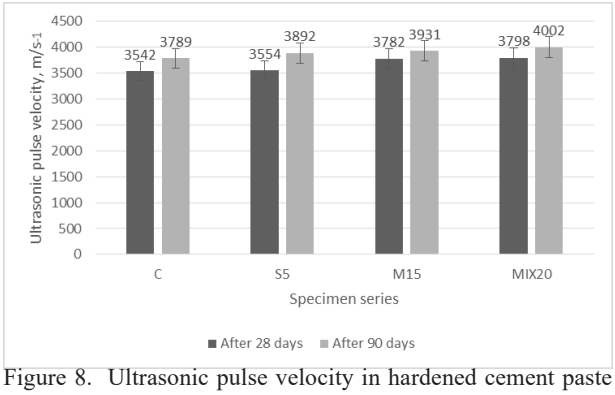

Figure 8. Ultrasonic pulse velocity in hardened cement paste at 28 and 90 days

X-ray tests, thermogravimetric analysis, density and ultrasonic pulse velocity tests of hardened cement paste specimens were supported microstructure analysis. The microstructure of the specimens was analysed by means of electronic microscope with image magnification of 2000 times (Figure 9). Figure 9a illustrates the microstructure of the control specimen with small pores and portlandite crystals visible. Figure 9b presents the SEM image of the specimen containing 5 % of ground waste glass. A glass particle surrounded by portlandite CH and calcium hydrosilicate C-S-H crystals is visible. A strong link between the crystals and the glass particle is observed. Figure 9c presents the macrostructure of hardened cement paste with glass foam waste. The image contains a porous foam glass splinter, the surface of which is closely connected to the cement matrix. The foam glass surface is rough, voids and cavities are filled with hydration products and cement matrix. CH and C-S-H hydration products visible on the contact zone have made the contact zone between the matrix and foam

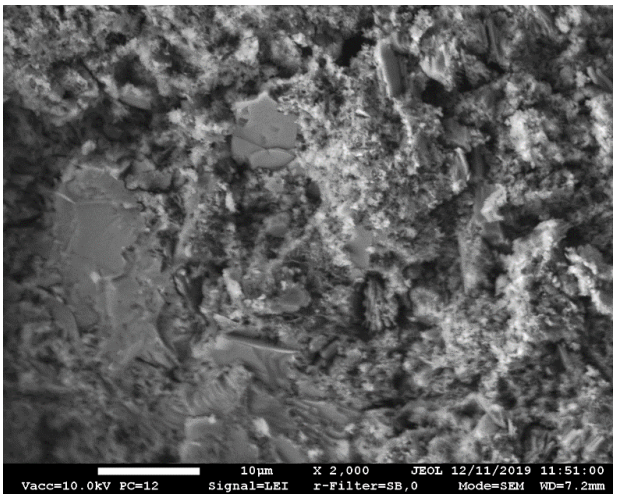

a) C

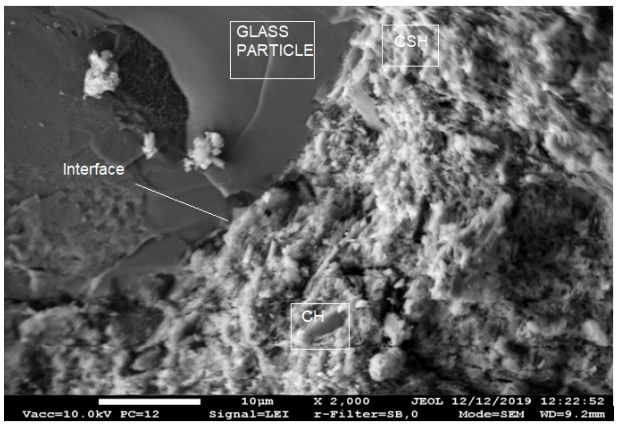

b) S 5

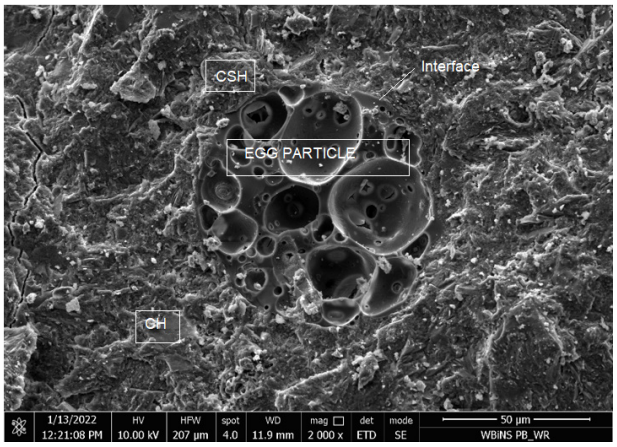

c) M 15

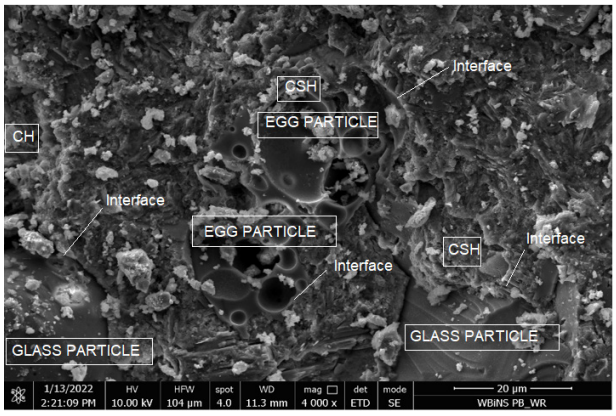

d) MIX 20

Figure 9. The microstructure of hardened cement paste.

glass particles stronger compared to the control specimen. Figure 9d presents the SEM image of hardened cement paste modified by a complex pozzolanic addition made of 5 % of ground glass powder and 15 % of metakaolin. The image shows glass particles and foam glass splinters with C-S-H crystals in the pores. The same hydration products and CH crystals are visible around the particles of foam glass and inactive glass. There is a strong link between cement matrices and inactive glass particles as well as foam glass splinters. Hydration products formed in the pores of foam glass splinters also make the hardened cement paste structure stronger.

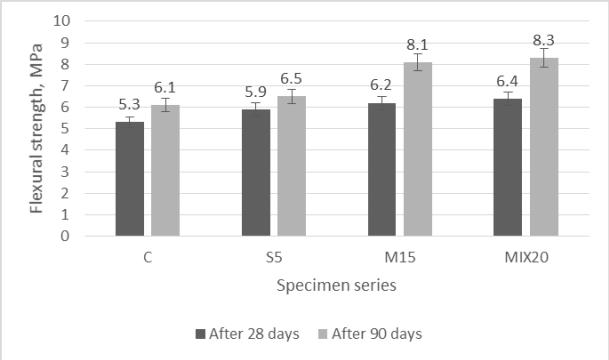

Figure 10. The bending strength of hardened cement paste at 28 and 90 days.

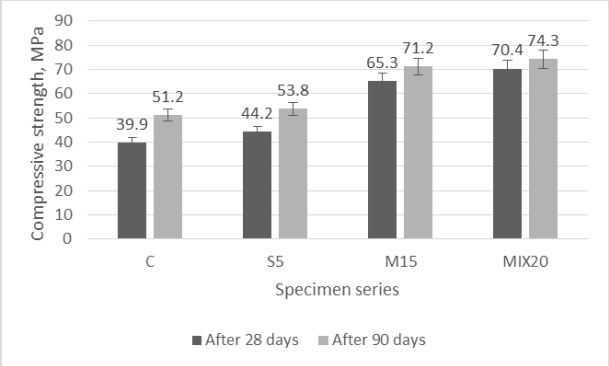

Figure 11. The compressive strength of hardened cement paste at 28 and 90 days

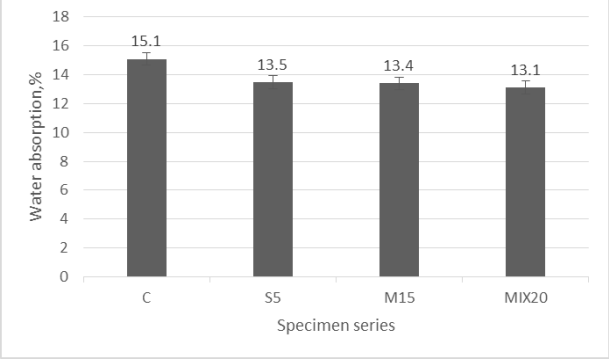

Figure 12. Water absorption in hardened cement paste.

The bending strength of hardened cement paste was measured after 28 and 90 days of curing (Figure 10). At 28 days the bending strength of control specimens was 5.3 MPa. In the specimens modified with 15 % metakaolin it increased to 6.2 MPa and in the specimens modified with 20 % of pozzolanic waste it reached 6.4 MPa, i.e. it was 17.19 % higher than in control specimens. At 90 days the bending strength of control specimens was 6.1 MPa and in the specimens modified with 20 % of pozzolanic waste (MIX 20) it was 8.3 MPa, i.e. it was 26.5 % higher than in control specimens.

At 28 days the compressive strength of control specimens was 39.9 MPa. It was 43.32 % higher in the specimens modified with 20 % of pozzolanic waste and reached 70.4 MPa (Figure 11). At 90 days the compressive strength of control specimens was 51.2 MPa and in the specimens modified with 5 % of ground waste glass and 15 % of metakaolin it was 74.3 MPa, i.e. 31.1 % than the compressive strength of control specimens. These tests supported the results of XRD tests and thermogravimetric analysis, showing that the specimens with a higher content of hydration products and higher strength values [42-44].

The water absorption test of hardened cement paste (Figure 12) showed that specimens MIX20, where cement was replaced with 5 % ground waste glass and 15 % of metakaolin. The highest water absorption of 15.1 % was observed in the specimens of control composition. The presumable cause of the highest water absorption is a more porous structure and lower density of those specimens. With a higher content of pozzolanic waste up to 20 %, the density of the specimens increases, the microstructure becomes more compact and the water absorption rate becomes 13.25 % lower than in control specimens.

CONCLUSIONS

Pozzolanic additions, such as ground waste glass and metakaolin used alone and in combination to modify hardened cement paste have a positive effect on the hardened paste's microstructure, intensify cement hydration, lead to the formation of new hydration products, and consequently improve physical and mechanical properties of hardened cement paste.

XRD tests showed that after 28 and 90 days of curing the amount of portlandite in modified specimens was lower than in control specimens, while the amount of secondary hydration products, such as C-S-H, increased. The biggest changes were observed in the specimens modified with 20 % of pozzolanic waste made of 5 % of ground waste glass and 15 % of metakaolin. A lower amount of cement in the mix leads to the reduction of portlandite in hardened cement paste, whereas pozzolanic reactions between free Ca(OH) and active glass and metakaolin addition produce more secondary hydration products.

X-ray analysis results supported by SEM tests confirmed that strong contact zones are formed between free glass particles and foam glass splinters present in metakaolin and strong cement matrices with a high amount of C-S-H minerals are formed in hardened cement paste where 20 % of cement is replaced by weight with a complex addition of pozzolanic waste.

The reduction of portlandite amount and increase of other reaction products in the specimens with pozzolanic addition was also confirmed by thermogravimetric analysis. The total mass loss in the control specimen was 13 % lower than in modified specimens. It means that additions intensify cement hydration.

Tests of physical and mechanical properties showed that density, ultrasonic pulse velocity, compressive and flexural strength increased in specimens with pozzolanic additions both at 28 and at 90 days. These properties increased in modified specimens due to more intensive hydration and the formation of a bigger amount of secondary hydration products. Water absorption rates were lower in the specimens modified with pozzolanic addition than in control specimens. The lowest water absorption rate was recorded in the specimens modified with 20 % of pozzolanic waste. It was 13.25 % lower than water absorption in control specimens. A lower water absorption rate in those specimens resulted from a denser microstructure of the hardened cement paste.

Modification of concrete mix with pozzolanic additions made of ground waste glass and metakaolin has a positive effect on the hardened paste's microstructure. Supplementary hydration products formed due to more intensive hydration improve the physical and mechanical properties of hardened cement paste.

REFERENCES

1. Kim S. K., Kang S.T., Kim J.K., Jang I. Y. (2017). Effects of Particle Size and Cement Replacement of LCD Glass Powder in Concrete. *Advances in Materials Science and Engineering, 2017*. doi:10.1155/2017/3928047
2. Punitha V., Sakthieswaran N, Babu O.G. (2021): Experimental investigation of concrete incorporating HDPE plastic waste and metakaolin.(2021). *Materials Today: Proceedings, 37*, 1032-1035. doi:10.1016/j.matpr.2020.06.288
3. Pastariya S., Lohar G. (2020). Effect of Metakaolin on Mechanical Properties on the Strength of Hardened Concrete for M-35 Concrete. doi:10.13140/RG.2.2.10167.14240
4. Ibrahim S.S., Hagrass A.A., Boulos T.R., Youssef S.I., El-Hossiny F.I., Moharam M.R. (2018): Metakaolin as an Active Pozzolan for Cement That Improves Its Properties and Reduces Its Pollution Hazard. *Journal of Minerals and Materials Characterization and Engineering, 6*, 86-104. doi: 10.4236/jmmce.2018.61008
5. Szudek W., Gołek Ł., Malata G., Pytel, Z. (2022): Influence of Waste Glass Powder Addition on the Microstructure and Mechanical Properties of Autoclaved Building Materials. *Materials, 15*, 434. doi:10.3390/ma15020434
6. Ilić B., Radonjanin V., Malešev M., Zdujić M, Mitrović A. (2016): Study on the addition effect of metakaolin and mechanically activated kaolin on cement strength and microstructure under different curing conditions. *Construction and Building Materials, 133*, 243-252. doi:10.1016/j.conbuildmat.2016.12.068
7. Chand G., Happy S.K., Ram S. (2021): Assessment of the properties of sustainable concrete produced from quaternary blend of portland cement, glass powder, metakaolin and silica fume. *Cleaner Engineering and Technology, 4* , 100179. doi:10.1016/j.clet.2021.100179
8. Bumanis G., Vitola L, Stipniece L., Locs J., Korjakins A., Bajare D. (2020): Evaluation of Industrial by-products as pozzolans: A road map for use in concrete production. *Case Studies in Construction Materials, 13*, 2214-5095. doi:10.1016/j.cscm.2020.e00424
9. Wang Y, Cao Y, Zhang P, Ma Y. (2020) : Effective Utilization of Waste Glass as Cementitious Powder and Construction Sand in Mortar. *Materials, 13*(3), 707.doi:10.3390/ma13030707
10. Ahmad J., Martínez-García R., de-Prado-Gil J., Irshad K., El-Shorbagy M.A., Fediuk R., Vatin N.I. (2022): Concrete with Partial Substitution of Waste Glass and Recycled Concrete Aggregate. *Materials, 15*, 430. doi:10.3390/ma15020430
11. Asa E., Anna, A.S., Baffoe-Twum, E. (2019): An investigation of mechanical behavior of concrete containing crushed waste glass. *Journal of Engineering, Design and Technology, 17*, 1285-1303. doi:10.1108/JEDT-01-2019-0020
12. Lu X.J, Poon C.S. (2019). Recycling of waste glass in construction materials. In: *New Trends in Eco-efficient and Recycled Concrete*, Woodhead Publishing. pp.153-167. doi:10.1016/B978-0-08-102480-5.00006-3
13. Bisikirske,D, Blumberga D., Vasarevicius S., Skripkiunas G. (2019): Multicriteria Analysis of Glass Waste Application. *Environmental and Climate Technologies, 23*(1), 152-167. doi:10.2478/rtuect-2019-0011
14. Ammari, M.S., Tobchi, M.B., Amrani, Y., Mim, A., Bederina, M. and Ferhat, A. (2021): Influence of glass powder incorporation on the physical-mechanical properties of sand concrete. *World Journal of Engineering*, article in press. doi:10.1108/WJE-08-2021-0474
15. Siddika A, Hajimohammadi A, Ferdous W, Sahajwalla V. (2021): Roles of Waste Glass and the Effect of Process Parameters on the Properties of Sustainable Cement and Geopolymer Concrete. Review. *Polymers, 13*(22), 3935. doi:10.3390/polym13223935
16. He Z.H., Zhan P. M., Du S.G., Liu B.J., Yuan W.B. (2019): Creep behavior of concrete containing glass powder. *Composites Part B: Engineering, 166*, 13-20. doi:10.1016/j.compositesb.2018.11.133
17. El-Diadamony H., et al. (2016). Hydration and characteristics of metakaolin pozzolanic cement pastes. *HBRC journal, 14*(2), 150-158. doi:10.1016/j.hbrcj.2015.05.005
18. Belebchouche C., Moussaceb K., Bensebti S. E., Aït-Mokhtar A., Hammoudi A., Czarnecki S. (2021): Mechanical and microstructural properties of ordinary concrete with high additions of crushed glass. *Materials, 14*(8), 1872. doi:10.3390/ma14081872
19. Vaitkevičius V., Šerelis E., Hilbig H. (2014): The effect of glass powder on the microstructure of ultra high performance concrete. *Construction and Building Materials, 68*, 102-

109. doi:10.1016/j.conbuildmat.2014.05.101
20. Vignesh K.S., Rajkumar R., Umamaheswari N. (2019): Study on mechanical and microstructure properties of concrete prepared using metakaolin, silica fume and manufactured sand. *Rasayan Journal of Chemistry, 12*(3), 1383-1389.doi: 10.31788/RJC.2019.1235164
21. Sá A. W. dos S. G. de, Coutinho Y., Soares R. G. P., Ferreira F. C., Carneiro A. M. P. (2021): Evaluation of compressive strength of concrete with metakaolin using different levelling techniques. *Research, Society and Development, 10*(3), e31510313341-e31510313341. doi:10.33448/rsd-v10i3.13341
22. Bheel N., Abbasi S.A., Awoyera P., Olalusi O.B., Sohu S., Rondon C., Echeverría A.M. (2020): Fresh and Hardened Properties of Concrete Incorporating Binary Blend of Metakaolin and Ground Granulated Blast Furnace Slag as Supplementary Cementitious Material. *Advances in Civil Engineering, 8*, 8851030. doi:10.1155/2020/8851030
23. Dinakar P., Sahoo P.K., Sriram G. (2013): Effect of Metakaolin Content on the Properties of High Strength Concrete. *International Journal of Concrete Structural Material, 7*, 215–223. doi:10.1007/s40069-013-0045-0
24. Park K. B., Lin R. S., Han Y., Wang X. Y. (2021): Model-Based Methods to Produce Greener Metakaolin Composite Concrete. *Applied Sciences, 11*(22), 10704. doi:10.3390/app112210704
25. Yue C. (2021): Low-carbon binders produced from waste glass and low-purity metakaolin for cemented paste backfill, *Construction and Building Materials, 312*, 125443. doi:10.1016/j.conbuildmat.2021.125443
26. Xupeng C., Zhuowen S., Jianyong P. (2021): Study on Metakaolin Impact on Concrete Performance of Resisting Complex Ions Corrosion. *Frontiers in Materials, 8*, 788079. doi: 10.3389/fmats.2021.788079
27. Pillay D.L., Olalusi O.B., Kiliswa M.W., Awoyera P.O., Kolawole J.T., Babafemi A.J. (2022): Engineering performance of metakaolin based concrete, *Cleaner Engineering and Technology, 6*, 100383. doi:10.1016/j.clet.2021.100383
28. Ouldkhaoua Y., Benabed B., Abousnina R., Kadri E. H. (2019): Rheological properties of blended metakaolin self-compacting concrete containing recycled CRT funnel glass aggregate. *Epitoanyag-Journal of Silicate Based & Composite Materials, 71*(5), 154–161. doi:10.14382/epitoanyag-jsbcm.2019.27
29. Du Y., Yang W., Ge Y., Wang S., Liu P. (2020): Thermal conductivity of cement paste containing waste glass powder, metakaolin and limestone filler as supplementary cementitious material. *Journal of Cleaner Production, 287*, 125018. doi:10.1016/j.jclepro.2020.125018
30. Zhang L., Lionel J.J., Catalan L.J.J., Andrew C., Larsen A.C.,Stephen D., Kinrade S.D.(2007): Effects of sucrose and sorbitol on cement-based stabilization/solidification of toxic metal waste. *Journal of Hazardous Materials, 151*, 490-498. doi:10.1016/j.jhazmat.2007.06.022
31. Shin S.M., Ho Ch. S., Song Y. Sh., Lin J.P. (1999): Kinetics of the Reaction of $Ca(OH)_2$ with CO_2 at Low Temperature *Industrial & Engineering Chemistry Research, 38*(4), 1316-1322. doi:10.1021/ie980508z
32. Jiahui P., Jianxin Z., Jindong, Q. (2006): The mechanism of the formation and transformation of ettringite. *Journal of Wuhan University of Technology-Mater. Sci. Ed., 21*(3), 158-161. doi: 10.1007/BF02840908
33. Hartmann M.R., Brady S.K., Berliner R., Conradi M.S. (2006): The evolution of structural changes in ettringite during thermal decomposition. *Journal of Solid State Chemistry, 179*(4), 1259-1272. doi: 10.1016/j.jssc.2006.01.038
34. Sha W., O'Neill E.A., Guo Z. (1999): Differential scanning calorimetry study of ordinary Portland cement. *Cement and Concrete Research, 29*(9), 1487-1489. doi: 10.1016/S0008-8846(99)00128-3
35. Gabrovšek R., Vuk T., Kaučič T.(2008): The Preparation and Thermal Behavior of Calcium Monocarboaluminate. *Acta Chimica Slovenica, 55*(4), 942-950.
36. Zhou Q., Glasser F.P. (2001): Thermal stability and decomposition mechanisms of ettringite at < 120 degrees C. *Cement and Concrete Research, 31*(9), 1333-1339. doi: 10.1016/S0008-8846(01)00558-0
37. Nonnet E., Lequeux N., Boch P. (1999): Elastic properties of high alumina cement castables from room temperature to 1600°C. *Journal of the European Ceramic Society, 19*(8), 1575-1583. doi:10.1016/S0955-2219(98)00255-6
38. Stepkowska E. T. (2006): Simultaneous IR/TG study of calcium carbonate in two aged cement pastes. *Journal of Thermal Analysis and Calorimetry, 84*(1), 175-180. doi: 10.1007/s10973-005-7179-5
39. Prince W., Espagne M., Aïtcin P. C. (2003): Ettringite formation: A crucial step in cement superplasticizer compatibility. *Cement and Concrete Research, 33*(5), 635-641. doi:10.1016/S0008-8846(02)01042-6
40. Khoury G.A.(1992): Compressive strength of concrete at high temperatures: a reassessment. *Magazine of Concrete Research, 44*(161), 291-309. doi:10.1680/macr.1992.44.161.291
41. Palou M.T., Kuzielova E., Novotny R., Šoukal F., Žemlička M. (2016): Blended cements consisting of Portland cement–slag–silica fume– metakaolin system. ournal of *Thermal Analysis and Calorimetry, 125*(3), 1025-1034. doi: 10.1007/s10973-016-5399-5
42. Szeląg M. (2020): Fractal characterization of thermal cracking patterns and fracture zone in low-alkalicement matrix modified with microsilica. *Cement and Concrete Composites, 114*, 1-14. doi:10.1016/j.cemconcomp.2020.103732
43. Mermerdaş K., İpek S., Algın Z., Ekmen S., Güneş I. (2020). Combined effects of microsilica, steel fibre and artificial lightweight aggregate on the shrinkage and mechanical performance of high strength ementitious composite. *Construction and Building Materials, 262*, 120048. doi:10.1016/j.conbuildmat.2020.120048
44. Gesoglu M., Güneyisi E., Assad, S., Muhyaddin G. (2016). Properties of low binder ultra-high performance cementitious composites: Comparison of nanosilica and microsilica. *Construction and Building Materials, 102*, 706-713. doi:10.1016/j.conbuildmat.2015.11.020.